Journal of Visualization, Vol.6, No.1 (2003) 41-51

Measurement on CO_2 Solution Density by Optical Technology

Song, Y.*[1], Nishio, M.*[2], Chen, B.*[1], Someya, S.*[2] and Ohsumi, T.*[1]

*1 Research Institute of Innovative Technology for the Earth (RITE), Tsukuba-division of RITE, East-Tsukuba, Tsukuba 305-8564, Japan. e-mail: b.chen@aist.go.jp
*2 National Institute of Advanced Industrial Science and Technology (AIST), East-Tsukuba, Tsukuba 305-8564, Japan.

Received 3 June 2002
Revised 8 October 2002

Abstract : The optical technology based on Mach-Zehnder interferometry was successfully applied to a high-pressure liquid CO_2 and water system to measure CO_2 solution density. Experiments were carried out at a pressure range of from 5.0 to 12.5 MPa, temperatures from 273.25 to 284.15 K, and CO_2 mass fraction in solution up to 0.061. CO_2 solution density data were obtained from two sets of experiments. These data were calculated through the fringe shifts induced by density changes inside of the high-pressure vessel, which were directly recorded during the experiments, and a modified version of Lorentz-Lorenz formulation. The experimental results indicated that the density ratio of CO_2 solution to that of pure water at the same pressure and temperature is monotonically linear with the CO_2 concentration in the solution. The slope of this linear function, calculated by the experimental data fitting, is 0.275.

Keywords: CO_2 solution, density, Mach-Zehnder Interferometry, CO_2 ocean sequestration.

Nomenclature

M : molar mass	[g/mol]
N : atomic number in unit volume	[-]
n : refractive index	[-]
Δn : difference of refractive indexes	[-]
P : pressure	[MPa]
R : molar refraction	[cm^3/mol]
Δs : fringe shift number	[-]
T : temperature	[°C]
α : electronic polarizability	[m^3]
δ : probing distance	[mm]
λ : laser wavelength	[nm]
ρ : density or bulk concentration	[g/cm^3]
χ : mass fraction	[-]
ε : dielectric constant	[-]

Subscript

a : state after CO_2 droplet injection
b : state before CO_2 droplet injection

c : CO_2
w: water
s : state of CO_2 droplet being completely dissolved
sl : solution

1. Introduction

Physicochemical properties of CO_2-water binary system have recently received growing experimental and theoretical interest due to the environment and climate related effects of greenhouse gases. Mitigating CO_2 gas emitted from burning fossil fuel and other major greenhouse gases (CH_4, N_2O, etc.) in the atmosphere now has become undoubtedly an urgent task aimed to stabilize the atmosphere concentration of greenhouse gases at a certain level and prevent dangerous disruption of the climate system. Among several options proposed, including biological sequestration, geological sequestration and ocean storage (Marchetti, 1997 and Steinberg et al., 1980), ocean sequestration appears to have the advantage of relative lower cost, high efficiency, large capability and limited environmental impact

There are two ideas for CO_2 ocean storage. One is the "dense ocean floor storage", by which a large amount of liquid CO_2 (LCO_2) could be stored in an ocean basin deeper than 3000 m where CO_2 density is larger than that of seawater (Aya et al., 1997). The other is the "middle depth dilution". At a depth about 1000 m, it was suggested by this technology that LCO_2 might be directly injected into the ocean by either a set of fixed nozzles or a way called "moving-ship" (Haugan et al., 1995 and Liro et al., 1992) to form two plumes of LCO_2 droplets and CO_2 enriched seawater. CO_2 droplets will dissolve into seawater as they rise up (positive buoyancy). By this way, it is expected that it might be possible to limit local CO_2 concentration at a controllable level to produce a minimum biological impacts (Nakashiki et al., 1995)

For both ideas, obviously, the fundamental knowledge of physical and chemical mechanism and properties of this CO_2-water system, e.g. hydrate formation mechanism, CO_2 solution density, solubility and surface tension, is indispensable for engineering design and for developing a reasonable numerical model to predict the ocean environmental impacts on CO_2 sequestration. CO_2 solution density is one of these properties. Since the buoyancy is one of the major forces for ocean dynamics, CO_2 solution density does not only govern the plume structure near the releasing nozzles but also the further evolution of CO_2 enriched plume in large scale (Haugan et al., 1992). However, there are few systematical CO_2 solution density data in the literature on low temperature and high pressure. For the gas CO_2 saturated solution, Parkinson et al (Parkinson et al., 1969) measured the densities at a pressure range of from 1.0 to 3.4 MPa with temperatures from 273.15 to 313.15 K. Their results at low temperatures (278 ~ 284.25K) show a decrease in solution density with an increase in pressure when the pressure is higher than 3.5 MPa. To measure CO_2 solubility for geological and natural gas engineering, Nighswander et al. (1989) added some new data at pressures from 2.0 to 10.0 MPa with temperatures from 353.15 to 473.15 K. With focusing on CO_2 ocean storage investigation, Ohsumi et. al. (1992) measured LCO_2 solution densities at low CO_2 concentrations by a vibration-density meter. Also for ocean storage on the basin (20 ~ 30 MPa), very recently Aya (2000) reported CO_2 solution density varied with respect to CO_2 mass fraction by using a weighting technology. By comparison with these two sets of data, Aya (2000) found out that the slope of density difference between CO_2 solution and water with respect to CO_2 mass fraction obtained from his experiments is 7.0 percentage smaller than that from Ohsumi's.

In this study, we report the last experimental results of CO_2 solution density at pressures and temperatures ranging from 5.0 to 12.5 MPa and 273.25 to 284.15 K, and CO_2 concentration (in mass fraction) up to 0.061. These experiments were carried out by using a high-pressure vessel with a standard safe pressure of 15.0 MPa and Mach-Zehnder Interferometry.

2. Measurement Methodology

The principle of measuring CO_2 solution density in this study is based on the method of Mach-Zehnder Interferometry. Figure 1 gives the schematic diagram of the experimental apparatus. The experimental system consists of mainly two parts. One is the optical system and the other is the CO_2 dissolution system. The laser used in this study is a D100E Pumped Crystal Laser (CL-100) with the power of 500mW and wavelength of 530nm. The high-pressure vessel is made of SUS 316 stainless steel and designed to withstand safely 15.0 MPa of pressure. Three circular windows with a diameter of 20.0 mm are placed on the vessel walls. Two of them are located to be opposite horizontally for optical measurement with a distance of δ=35.0mm and the other is a window for monitoring , which is perpendicular to the measurement windows at the same horizontal level. These optical windows are made of Sapphire glass. The temperature of water or CO_2 solution inside the vessel can be adjusted from 263.15 K to 340.15 K by a heat exchanger with fluctuations less than $\pm$ 0.2 K. To enhance CO_2 dissolution and to maintain CO_2 solution inside the vessel in a homogeneous state, a stirrer was installed at the bottom of the vessel. The stirring strength can be adjusted at 10 different levels. Liquid CO_2 is injected into water or solution by an up-down nozzle with an inner-diameter of 1.3 mm to form a droplet. Because of the density difference between liquid CO_2 and water ($\rho_c<\rho_w$), this injected droplet was kept steadily hanging on the nozzle exit while dissolving into surrounding water or solution.

The fundamental principle of Mach-Zehnder Interferometry is to make use of the physical phenomenon of the difference of refractive index indicated by the interference from two identical laser beams, which are divided by a half-silvered mirror. One probing beam passes through the test vessel of CO_2 solution and the other is a reference beam. Interfere fringes appeared on the screen shift with density changes inside the vessel due to CO_2 injection and dissolution. A CCD camera (DXC-LS1 Sony) and a digital video (DCR-PC100, Sony) are used to record continually both of these interfere-fringe shifts and the dissolution process of CO_2 droplet injected. The interfere-fringe shifts will be counted later for calculating the density changes.

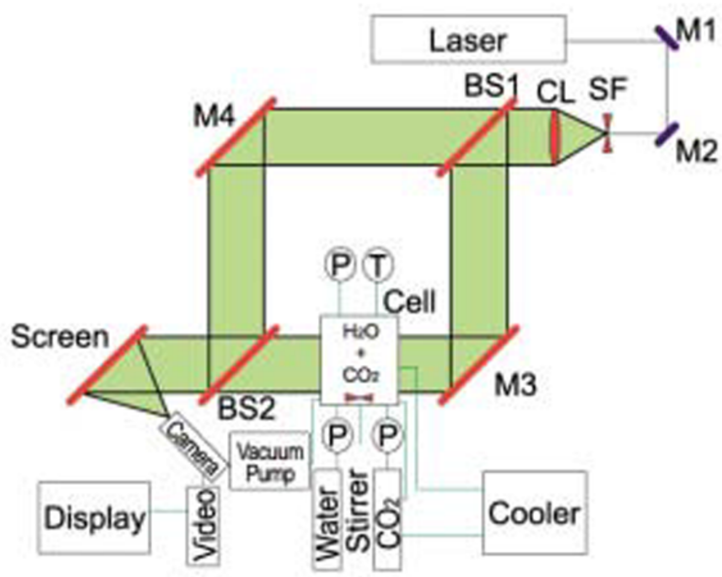

Fig. 1. Schematic diagram of experiment apparatus.

From optical physics, we can relate the fringe shift between the CO_2 solution and the fresh water, ΔS, to the difference of refractive indexes, Δn, by:

$$\Delta n\delta = (n_{sl} - n_w)\delta = \lambda \Delta s \tag{1}$$

through probing distance (δ), laser wave length (λ), and refractive indexes (n) of solution and water, respectively. For a pure substance, we have the Lorentz-Lorenz formulation (Koube, 1977):

$$\frac{n_i^2 - 1}{n_i^2 + 2} = \frac{R_i}{M_i}\rho_i \tag{2}$$

It must be noted that Eq. (2), the Lorentz-Lorenz formulation, is applicable for, in strictly speaking, perfect gases. However, according to the discussion from Born and Wolf (1959), they stated : "The molar refractivity is also found to remain practically constant when the gas is condensed into a liquid." Furthermore, the Chemical Handbook (Ito, 1984) introduced that Eq. (2) can be directly applied to liquids. In order to confirm the validity of using Eq. (2) in our experiment, we performed a calibration experiment for pure water by using Eqs. (1) ~ (2). The results are listed in Table 1. In this experiment, the pressure (0.1 ~ 11.89 MPa), temperature (kept in 4.6 °C), and fringe shift (ΔS) are measured from the calibrating experiment directly, while the densities and the initial refractive index (n_0=1.3342 for the start point at pressure of 0.1 MPa) are the data obtained from Handbooks (Lide, 1998-1999; Uchida, 1982), respectively. The refractive index n from the second point to the end is calculated by ΔS and Eq. (1) according to the relation:

$$n_k = n_{k-1} + \Delta n_k \tag{3}$$

$$\Delta n_k = \Delta S_k \frac{\lambda}{\delta} \tag{4}$$

where subscript k is the experimental number from 1 to 12. Then, molar refractivity, R_w, is calculated (the last column in Table 1). From this result, we evidenced the conclusion that Eq. (2) is adequately applied to liquids, especially to water, and the molar refractivity of water remains a constant of 3.715, which is slightly different with the value of 3.71 from theories (Ito, 1984). By using the molar refractivity of 3.71, we calculated in reverse the water density and found that the error produced are neglectfully small.

Having been evidenced, following relations can be derived straightforwardly for pure water and CO_2 from Eq. (2):

$$\frac{n_w^2 - 1}{n_w^2 + 2} = \frac{R_w}{M_w}\rho_w \tag{5}$$

$$\frac{n_c^2 - 1}{n_c^2 + 2} = \frac{R_c}{M_c}\rho_c \tag{6}$$

According to Maxwell electric-magnetic theory (Feynman et al., 1965):

$$3\left(\frac{n^2 - 1}{n^2 + 2}\right) = \sum_i N_i \alpha_i \tag{7}$$

we have the equations for CO_2-water binary system:

Table 1 The Lorentz-Lorenz Relation for Pure Water (Calibration in this experiment).

Pressure (MPa)	k	Temperature (°C)	Density ρ (g/cm³)	Fringe shift ΔS	Refractive index N	Molar refractivity R_w
0.1	0	4.6	0.99995	0	1.3342	3.7148
1.17	1	4.6	1.00046	13	1.33443	3.7152
2.13	2	4.6	1.00093	23	1.33461	3.7153
2.99	3	4.6	1.00134	33	1.33478	3.7155
4.01	4	4.6	1.00183	43	1.33496	3.7155
5.05	5	4.6	1.00233	53	1.33513	3.7154
6.07	6	4.6	1.00282	64	1.33533	3.7155
7.03	7	4.6	1.00328	74	1.3355	3.7156
8.16	8	4.6	1.00383	85	1.3357	3.7155
9.15	9	4.6	1.0043	95	1.33587	3.7155
10.16	10	4.6	1.00479	104	1.33603	3.7153
11.14	11	4.6	1.00526	114	1.33621	3.7153
11.89	12	4.6	1.00562	123	1.33637	3.7156

$$3\left(\frac{n_{sl}^2-1}{n_{sl}^2+2}\right)=\left(\sum_i N_i\alpha_i\right)_c+\left(\sum_i N_i\alpha_i\right)_w=3\left(\frac{n_c^2-1}{n_c^2+2}\right)+3\left(\frac{n_w^2-1}{n_w^2+2}\right) \quad (8)$$

then finally we obtain the equation related densities to refractive index of solution:

$$\frac{n_{sl}^2-1}{n_{sl}^2+2}=\frac{n_c^2-1}{n_c^2+2}+\frac{n_w^2-1}{n_w^2+2}=\frac{6.68}{44}\rho_c+\frac{3.71}{18}\rho_w \quad (9)$$

which is one of the key equations applied in this experiment. By coupling Eqs. (1) and (9), CO_2 solution refractive index, n_{sl}, and CO_2 density, ρ_c, (the actual bulk CO_2 concentration inside the vessel) can be obtained since fringe shifts due to density changes can be directly counted from those digital video records and other parameters appearing in these two equations, (water density, probing distance, laser wave-length, and refractive index of water) are all known. Consequently, the bulk CO_2 solution density and CO_2 mass fraction are obtained by:

$$\rho_{sl}=\rho_c+\rho_w \quad (10)$$

$$\chi=\frac{\rho_c}{\rho_{sl}}=\frac{\rho_c}{\rho_c+\rho_w} \quad (11)$$

3. Experiment Procedure

Before the experiment, the high-pressure vessel vacuumed up was fed with fresh water to an initial pressure and removed as much air as possible. This prepared high-pressure vessel was maintained for 24 hours for a preliminary leakage test by monitoring inside water pressure unchanged. As the first step, an individual liquid CO_2 was injected into the fresh water inside the vessel at a temperature of 279.15 K and pressure of 5.0 MPa, by which the initial density of the fresh water is determined. Once this injected liquid CO_2 droplet was completely dissolved up (The pressure decreased from that at the end of the droplet injection because of dissolution.), another droplet was injected again. This injection and dissolution process for an individual CO_2 droplet is called as “one step”. The experiment was progressed step by step repeatedly until the solution approached to the solubility limit. This entire process was continually monitored by a digital video for recording interfere-fringe shifts and liquid CO_2 droplets dissolution and by pressure and temperature sensors for detecting the thermodynamic state variation. For one step, the pressure and temperature of the fresh water or CO_2 solution at the starting time of liquid CO_2 injection were defined as T_b and P_b and those at the time of the end of injection were T_a and P_a, respectively. The pressure variation recorded from the experiment is shown in Fig. 2 for three steps (i−1, i, and i+1). These data were further used to estimate liquid CO_2 mass injected with the help of droplet volume recorded by CCD camera as additional reference to the result from Eq. (9). Because the liquid CO_2 dissolution rate lowered down as the experiment progressed, this experiment totally took about 5 days.

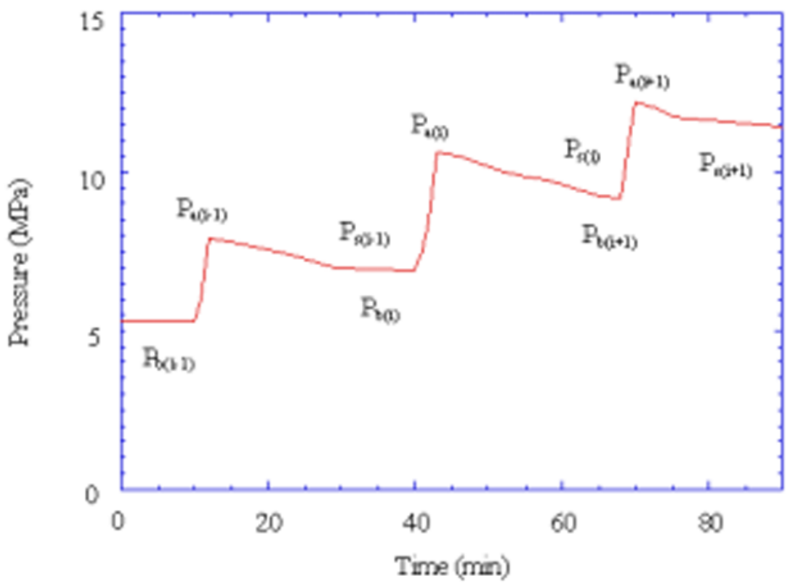

Fig. 2. Pressure variation during CO_2 droplet injection and dissolution.

The time evolution of a typical CO_2 droplet dissolving into solution sampled from continuous digital video records is shown in Fig. 3 as an example. The number of fringe shifting into or out of the screen due to the density changes and also due to the CO_2 injections can be easily counted from these digital video records.

At the moment for each step when CO_2 droplet was completely dissolved as shown in Fig. 3 (T=175 min.) with CO_2 solution (without any unsolved CO_2 coexists) inside the vessel having been stirred in an approximately homogenous state, interfere-fringe shifts from the beginning of injection

(Fig. 3 T=0) were counted from digital video records directly. By implementing these interfere-fringe shifts, pressure and temperature, and other property parameters required into Eq. (1) and Eqs. (9)~(11), CO_2 solution density and CO_2 concentration at each step were obtained progressively.
Additionally, it was noted from the experiment occasionally, when stirring was switched off, that a natural convection boundary was detected at the interface between CO_2 droplet and solution, which was produced by local density difference and dissolution. Though the attention of current study was paid to the vessel bulk density rather than the density field, it shed a light on understanding the mass transfer mechanism to further visualize the inner structure of this density boundary layer.

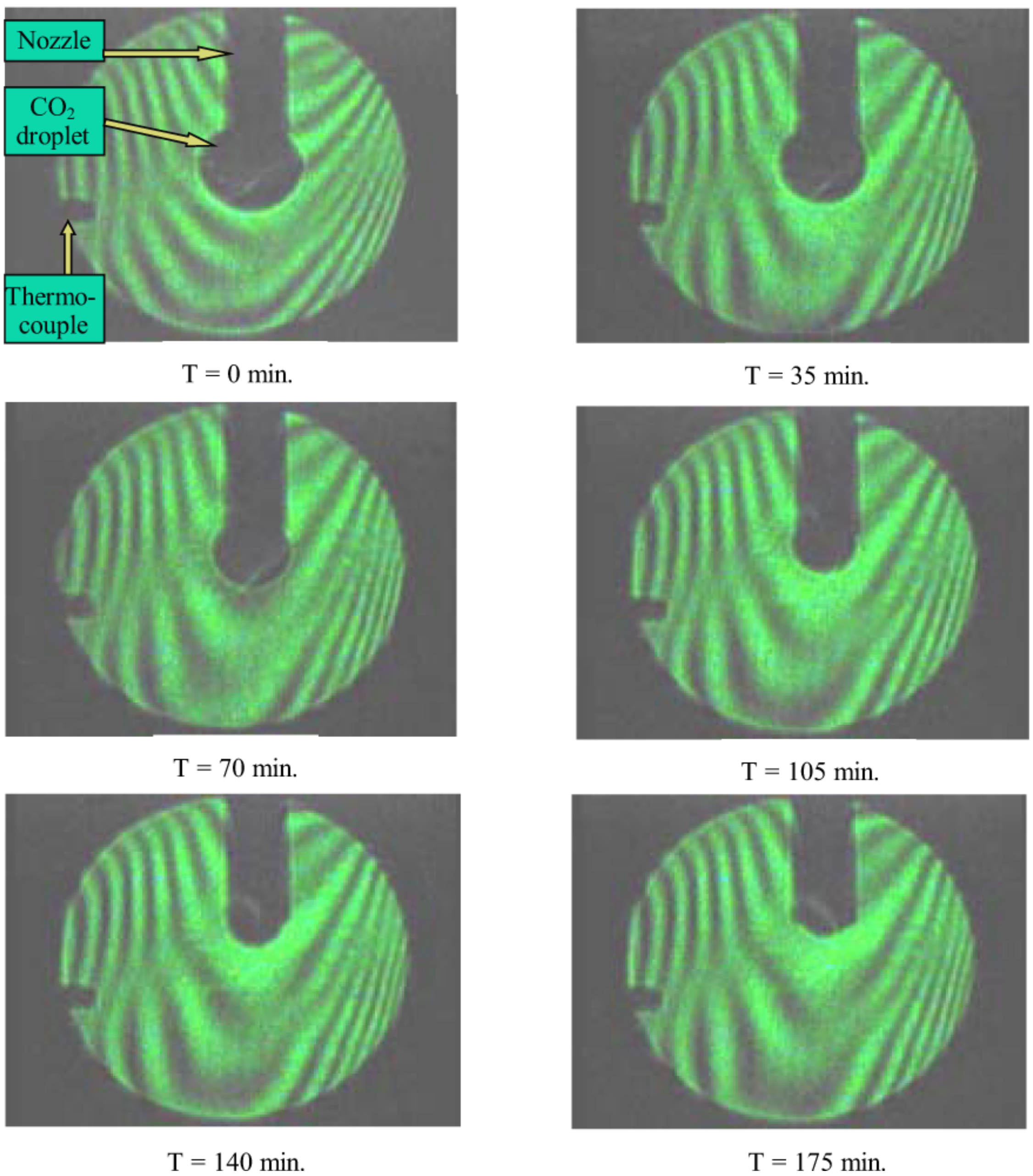

Fig. 3. Time evolution of a CO_2 droplet dissolution in water.

4. Results and Discussions

Two sets of data were obtained for experimental conditions at pressures ranging from 5.0 to 12.5 MPa, temperatures from 273.25 to 284.15 K, and CO_2 mass fraction in water up to 0.061. These data indicate that CO_2 solution density is nonlinearly proportional to the CO_2 mass fraction as shown in Fig. 4. For experiment-1, the initial pressure and temperature are 5.0 MPa and 279.15K, respectively. The solution pressure increased to 12.5 MPa as more CO_2 dissolved while the temperature was adjusted independently from 279.15K to 273.25K. For experiment-2, the initial sate was set at a relatively high temperature (284.15K) and low pressure (0.7 MPa). With keeping the temperature at initial one, the solution pressure increased to 9.0 MPa when the solution approached to solubility. From these data, it can be undoubtedly concluded only that CO_2 solution bears a nonlinear state relationship with density, pressure, temperature, and CO_2 mass fraction. However, when CO_2 solution density is normalized by pure water density at the same pressure and temperature, the state relationship becomes to be simple and clear version. As shown in Fig. 5, the ratio of CO_2 solution density to that of pure water at the same pressure and temperate, or the difference between these two densities, appears to be a monotonically linear relation with CO_2 mass fraction and seems to be independent of pressure and temperature at the experimental conditions listed here. The slope of this linear function, 0.275 was calculated by data fitting. This simple relationship is expressed by a state equation as the following :

$$\varphi = \rho_{sl} / \rho_w = 1.0 + 0.275\chi \tag{12}$$

This state equation is convenient to implement the numerical modeling code. For CO_2 ocean sequestration, as mentioned above, this linear relation indicates extensively that the additional negative buoyancy induced by CO_2 dissolution appears to be a constant, if CO_2 mass fraction is at the same value, and independent of the ocean depth (pressure and temperature). This also confirms the estimation that CO_2 enriched water will break down the original ocean stratification state and produce an additional gravity wave.

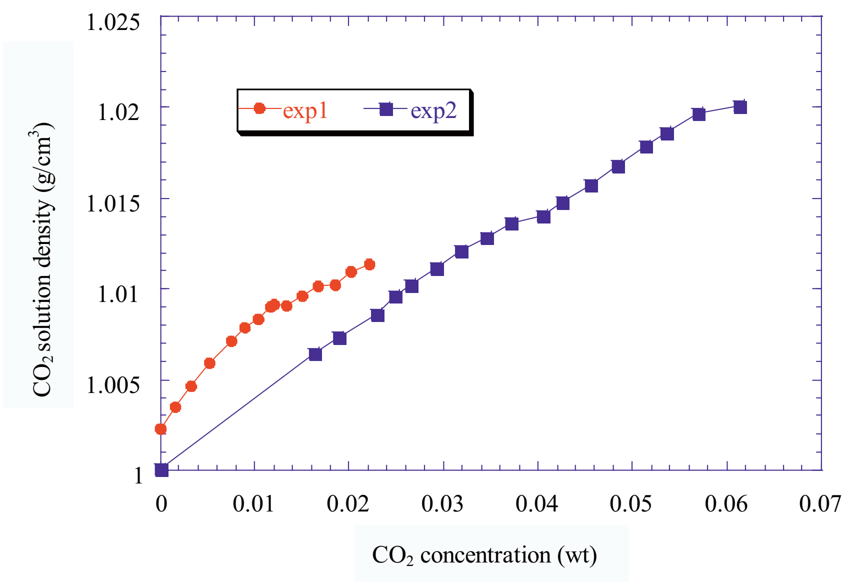

Fig. 4. CO_2 solution density for two sets of experiment.

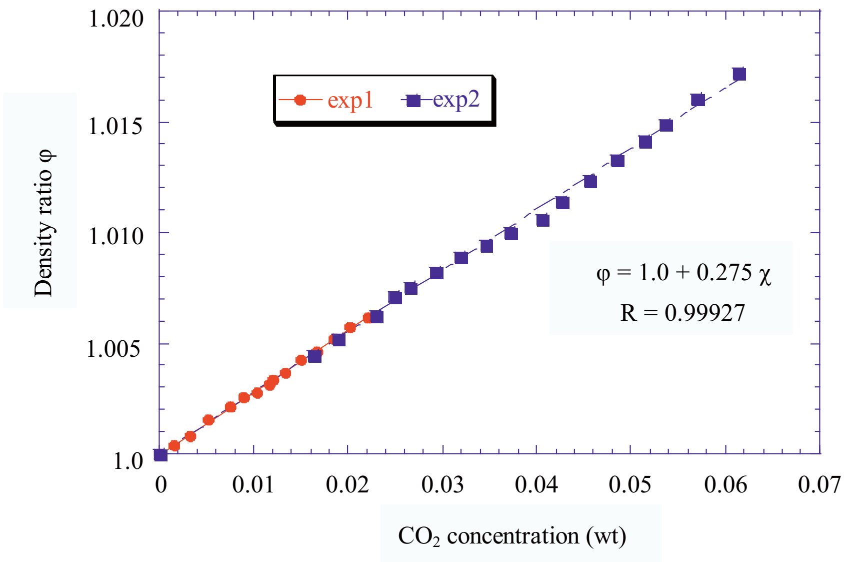

Fig. 5. Density ratio of CO_2 solution to pure water as the function of CO_2 concentration.

The mechanism of increasing CO_2 solution density while CO_2 is gradually dissolved into the water may be expressed by the interaction between water and CO_2 molecules. In the fact of the molecular structure, the size of CO_2 molecular is smaller than the distance between two water molecules, which allows the former to penetrate into the gaps between water molecules as they dissolved. Furthermore, the molecular density of CO_2 solution becomes larger than that of pure water and leads the CO_2 solution density to increase. It is also interesting to look at the pressure variations from the state of the beginning of liquid CO_2 injection, P_b, to the end of injection, P_a, and then the completely dissolved state, P_s. They have a relation, $P_b < P_s < P_a$ (Fig. 2), which implies that the volume of CO_2 solution is less than the individual volume of pure water plus pure CO_2 at the same state. It also means that the distance between water molecules increases when CO_2 is dissolved into water.

In addition to the experimental error involved in temperature and pressure measurement, one uncertainty to be considered is the interfere-fringe shift resolution created on the screen and the other is the expansion of probing distance (δ) when the pressure increased. The entire error for the slope of Eq. (12) we estimated from the system calibration experiment should be within ±1.5 percentage.

5. Summery

CO_2 solution density is successfully measured by using a high-pressure dissolution vessel and Mach-Zehnder interferometry experimental system. The experimental data obtained were at a pressure range of from 5.0 to 12.5 MPa, temperature from 273.25 to 284.15 K, and CO_2 mass fraction in the solution up to 0.061. A new version of Lorentz-Lorenz formulation for liquid solution was derived from Maxwell electric-magnetic theory. By using this new equation, CO_2 solution density and CO_2 mass fraction in the solution can be directly estimated by the recorded fringe shifts induced by density changes. The experimental results indicate that the linear relation between the density ratio of CO_2 solution to that of pure water and CO_2 mass fraction has a slope of 0.275.

Acknowledgements

This study is a part of the investigation of the CO_2 Ocean Sequestration Project managed by Research Institute of Innovative Technology for the Earth (RITE) and funded by New Energy and Industrial Technology Development Organization (NEDO), Japan.

References

Aya, I., Direct Measurement on CO_2 Solution Density in the Hydrate Region, Proc. Japanese Chemical Engineering Symp. Miyazaki, (2000), 17(in Japanese).

Born, M. and Wolf, E., Principle of Optics, Pergamon Press (1959), 87.

Feynman, R.P, Leighten, R.B, and Sands, M. L., The Feynman Lectures on Physics, Edison-Wesley Pub. Comp. (1965).

Haugan, P. M., Thorkildsen, F. and Alendal, G., Dissolution of CO_2 in the Ocean, Energy Conservation Management, 36 (1995), 461-466.

Haugan, P. M. and Drange, H., Sequestration of CO_2 in the Deep Ocean by Shallow Injection, Nature, 357 (1992), 318-320.

Ito, M., Chemical Handbook, 3rd Ed., Maruzen Pub. Comp., Tokyo, (1984), 553-558.

Koube, K., Light and Molecule, Kyoritsu Pub. Comp., Tokyo, (1977).

Lide, D. R., CRC Handbook of Chemistry and Physics, 79th Ed. CRC Press, (1998-1999), 10-218.

Liro, C.R., Adams, E.E. and Herzog, H. J., Modeling the Release of CO_2 in the Deep Ocean, Energy Conservation management, 33 (1992), 667-674.

Marchetti, C., On Geoengineering and the CO_2 Problem, Climate Change, 1 (1997), 59-68.

Nakashiki, N., Ohsumi, T. and Katano, N., Technical View on CO_2 Transportation on the Deep Ocean Floor and Dispersion at Intermediate Depth, In: Direct Ocean Disposal of Carbon Dioxide, Handa, N. and Ohsumi, T. Eds. (1995), 183, TERREPUB Tokyo.

Nighswander, J. A., Kalogerakis, N. and Mehrotra, A.K., Solubilities of Carbon Dioxide in Water and 1% wt NaCl Solution at Pressure Up to 10MPa and Temperature from 80 to 200℃, J. Chem. Eng. Data., 34 (1989), 355-360.

Ohsumi, T., Nakashiki, N., Shitashima, K. and Hirama, K., Density Change of Water Due to Dissolution of Carbon Dioxide and Near Field Behavior of CO_2 from a Source on Deep-sea Floor, Energy Conservation management, 33 (1992), 685-690.

Parkinson, W. J., Nevers, N. D., Partial Molal Volume of Carbon Dioxide in Water Solution, Ind. Eng. Chem. Fundam., 8 (1969), 709-712.

Steinberg, M., Chen, H.C., and Horn, F., Brookhaven Nat. Labo. Rep. OE/CH/00016, (1980), Upton, N.Y.

Uchida, H. JSME Data Book: The Thermophysical Properties of Fluids, Meizen Pub. Lt. (1982), 210.

Author Profile

Yongchen Song: He received his MSc (Eng) and Ph.D. in Mechanical Engineering in1989 and 1992 respectively from Dalian University of Technology. He then was pointed as an academic staff of the University till the year of 1996 when he began to work in Nagoya University and National Environmental Institute Japan as a researcher. Since year 2000, he had been worked for Research Institute of Innovative Technology for the Earth (RITE), Japan as a senior researcher. His research interests are the investigations of optical-based diagnostics on fluid follows and on physic-chemical properties of fluids, CO_2 sequestration technology and Crystal Growth of Gas Hydrate.

Masahiro Nishio: He received his MSc (Eng) in Chemical Engineering in1987 from Yokohama National University. He also received Ph.D. in Chemical Engineering in 1990 from Yokohama National University, then worked as a researcher for Mechanical Engineering Laboratory, AIST, MITI. He has been working in the National Institute of Advanced Industrial Science and Technology (AIST) Tsukuba as a senior research scientist. His research interests are CO_2 sequestration technology, Crystal Growth of Gas Hydrate and Flow Visualization.

Baixin Chen: He received his Ph. D. degree in Mechanical Engineering in 1989 from Dalian University of Technology, then worked as an academic staff in the University till 1998 when he turned to work for Research Institute of Innovative Technology for the Earth (RITE), Japan. His research interests include the numerical simulation of turbulent multi-phase flows and Large-eddy simulation of environmental flows. He also interested in the optical diagnostics on physic-chemical properties of fluids and study of CO_2 hydrate clathrate formation and dissolution.

Satoshi Someya : He received his Ph. D. degree in Nuclear Engineering in 1998 from University of Tokyo, then worked as a Research Fellow of New Energy and Industrial Technology Development Organization (NEDO) (1998-2000) in the Mechanical Engineering Laboratory of AIST. He has worked in National Institute of Advanced Industrial Science and Technology (AIST) Tsukuba as a temporary researcher. He is a member of Thermal Engineering Research Group. His research interests are Crystal Growth, CO_2 sequestration, Flow Induced Vibration and Flow Visualization.

Takashi Ohsumi: He is currently Chief Researcher of Research Institute of Innovative Technology for the Earth (RITE) CO_2 Sequestration Research Group, on leave from Central Research Institute of Electric Power Industry (CRIEPI), Japan. In 1986, when working with Tokyo Institute of Technology, he was sent to Lake Nyos in Cameroon as a member of Japanese scientific mission to investigate the CO_2 eruption disaster. In 1983 he received Ph. D. in Chemical Oceanography from University of Tokyo.